

Azaindole-1,2,3-triazole conjugate as selective fluorometric sensor for dihydrogenphosphate

Kumares Ghosh^{*a}, Debasis Kar^a, Soumen Joardar^a, Debashis Sahu^{b,c}, Bishwajit Ganguly^{*b,c}

^aDepartment of Chemistry, University of Kalyani, Kalyani, Nadia-741235, India, Email: ghosh_k2003@yahoo.co.in, ^bComputation and Simulation Unit (Analytical Discipline and Centralized Instrument Facility), CSIR-Central Salt and Marine Chemicals Research Institute, Bhavnagar, Gujarat, 364002. ^cAcademy of Scientific and Innovative Research; CSIR- Central Salt and Marine Chemicals Research Institute, Bhavnagar, Gujarat, 364002, India.

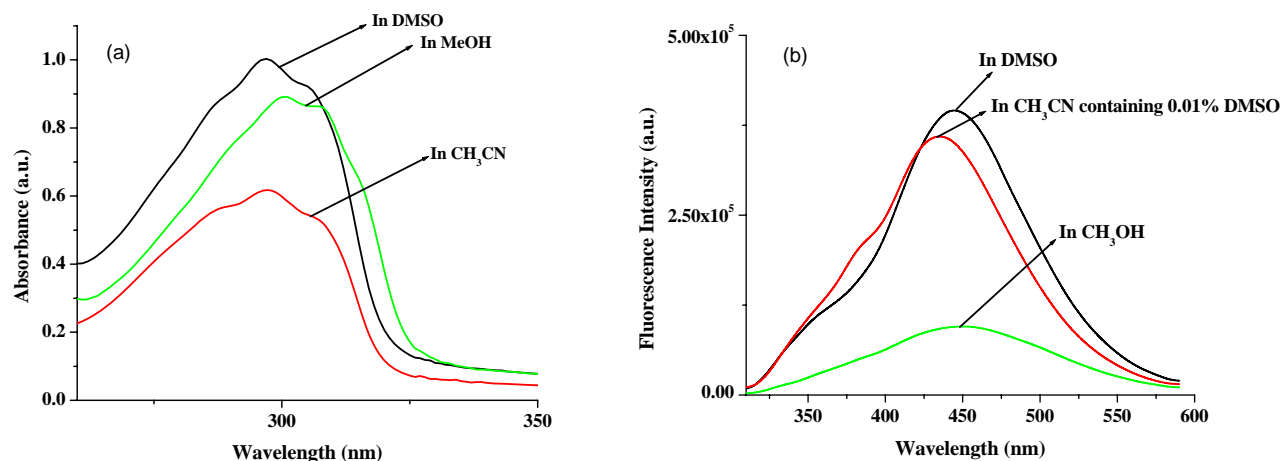


Figure 1S. (a) Absorption and (b) emission spectra of **3** ($c = 3.09 \times 10^{-5}$ M) in different solvents.

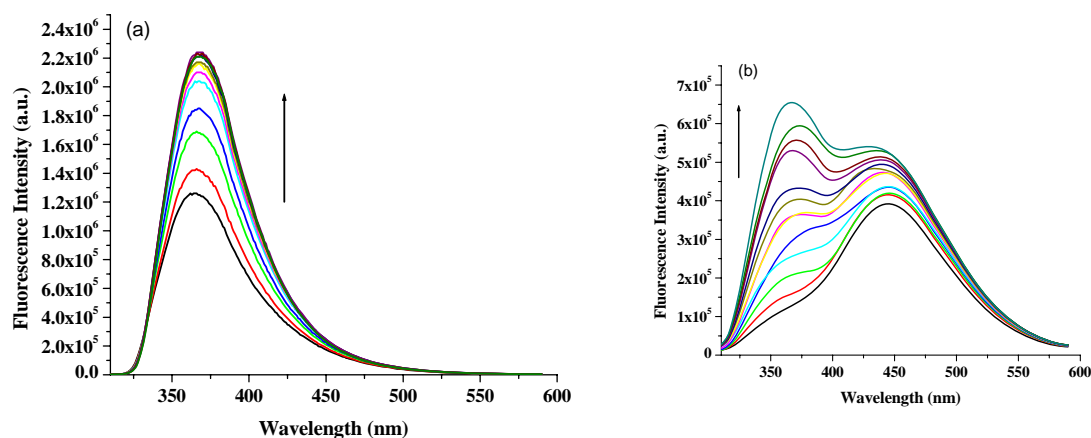


Figure 2S. Change in emission of (a) **1** ($c = 3.23 \times 10^{-5}$ M) and (b) **3** ($c = 4.25 \times 10^{-5}$ M) upon titration with DMSO in CH₃CN containing 0.01% DMSO.

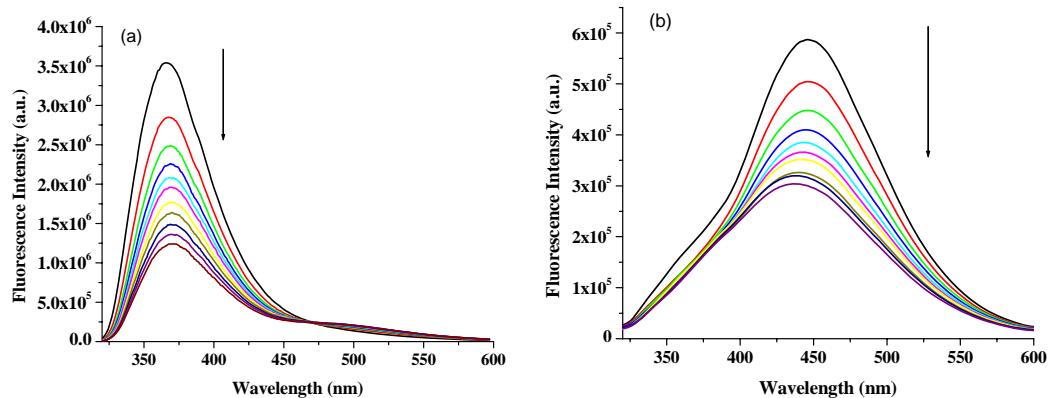


Figure 3S. Change in emission of (a) **1** ($c = 3.25 \times 10^{-5} \text{ M}$) and (b) **3** ($c = 3.09 \times 10^{-5} \text{ M}$) upon titration with CH_3OH in CH_3CN containing 0.01% DMSO.

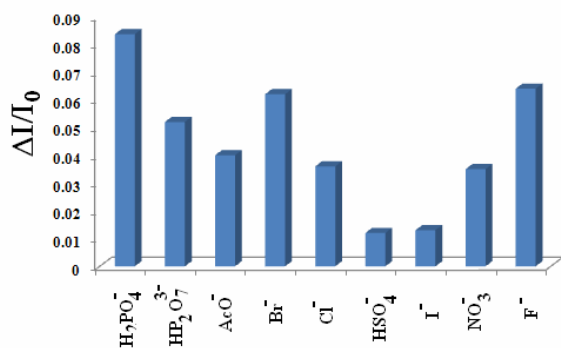


Figure 4S. Change in fluorescence ratio of **1** ($c = 4.52 \times 10^{-5} \text{ M}$) at 370 nm upon addition of 15 equiv. amounts of different guests in DMSO.

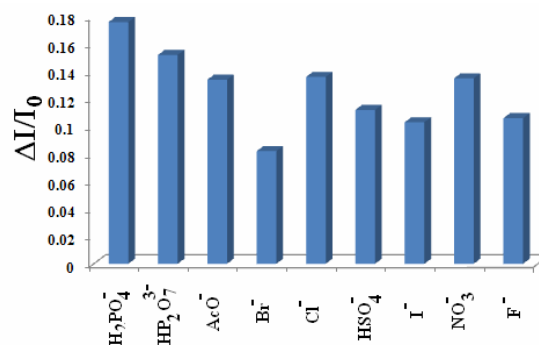


Figure 5S. Change in fluorescence ratio of **3** ($c = 3.45 \times 10^{-5} \text{ M}$) at 370 nm upon addition of 15 equiv. amounts of different guests in DMSO.

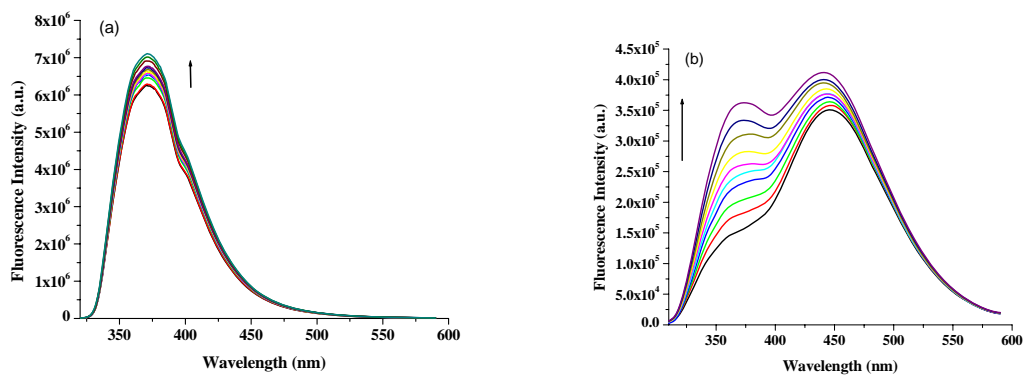


Figure 6S. Change in emission of (a) **1** ($c = 4.52 \times 10^{-5} \text{ M}$) and (b) **3** ($c = 3.63 \times 10^{-5} \text{ M}$) when titrated with H_2PO_4^- ($c = 1 \times 10^{-3} \text{ M}$) in DMSO.

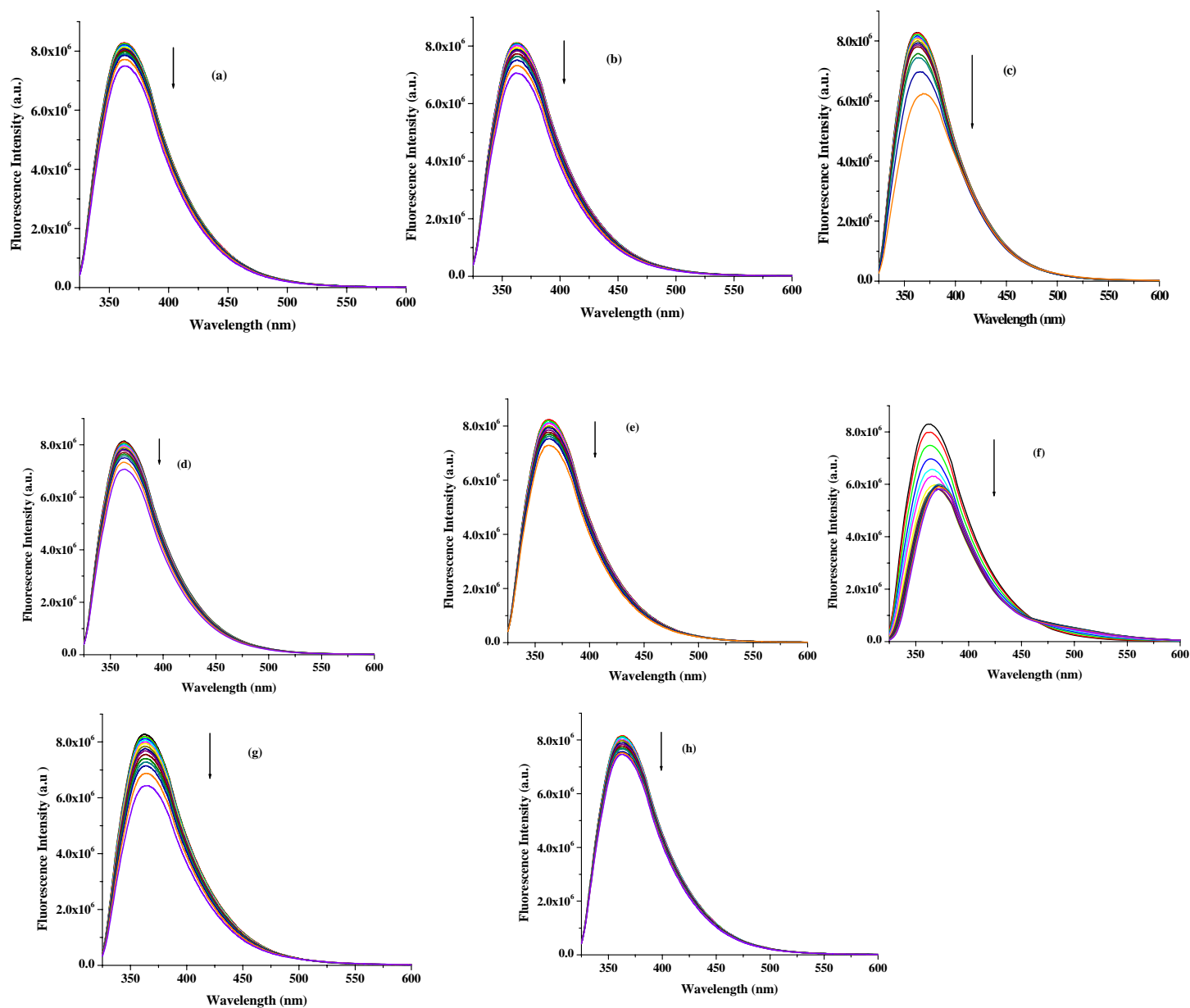


Figure 7S. Change in emission of **1** ($c = 2.51 \times 10^{-5} \text{ M}$) upon addition of a) Cl^- , b) Br^- , c) F^- , (d) I^- , e) HSO_4^- , (f) $\text{HP}_2\text{O}_7^{3-}$, (g) AcO^- , (h) NO_3^- in CH_3CN containing 0.01% DMSO.

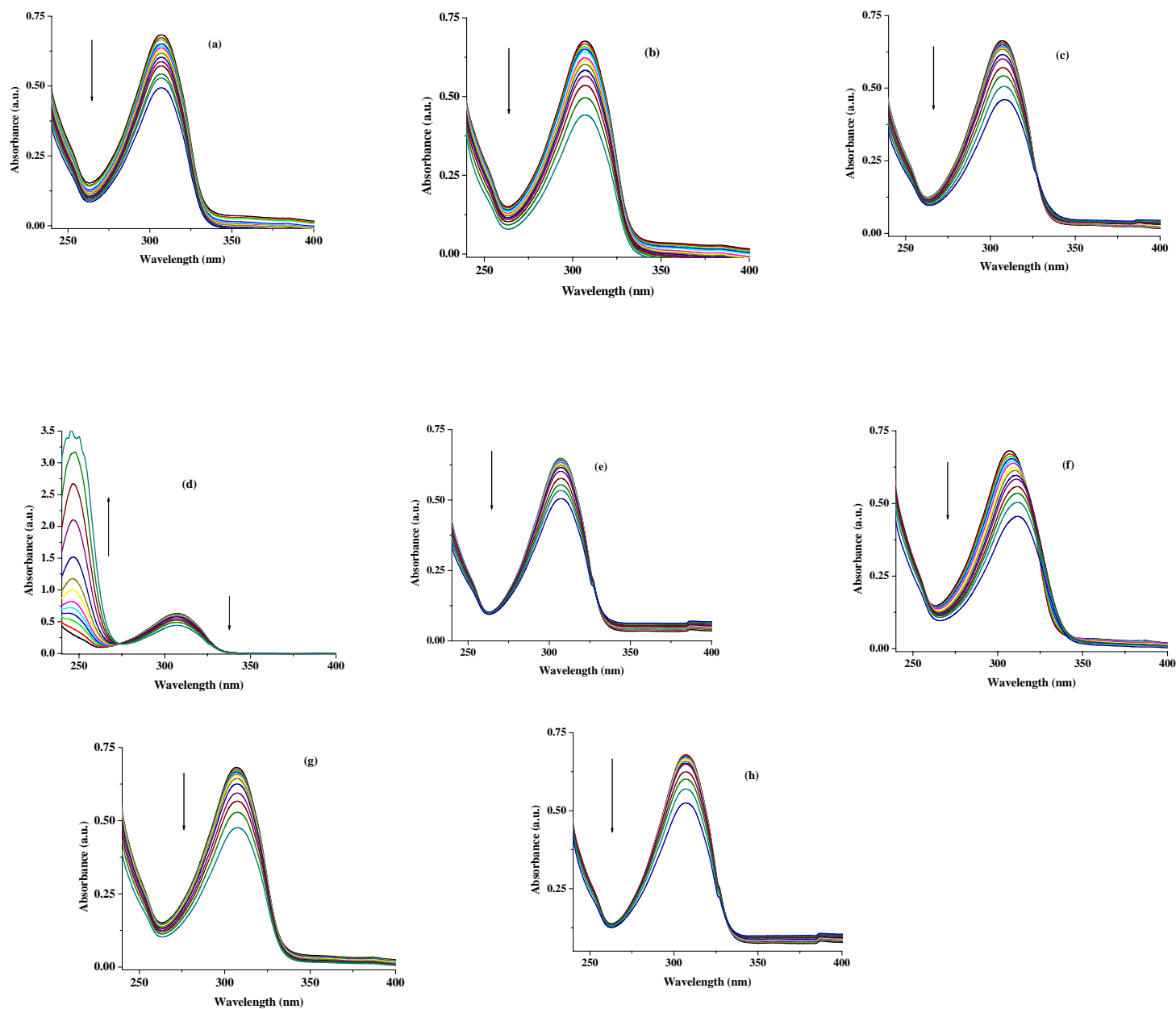


Figure 8S. Change in absorbance of 1 ($c = 2.51 \times 10^{-5} \text{ M}$) upon addition of a) Cl^- , b) Br^- , c) F^- , (d) I^- , e) HSO_4^- , (f) $\text{HP}_2\text{O}_7^{3-}$, (g) AcO^- , (h) NO_3^- in CH_3CN containing 0.01% DMSO.

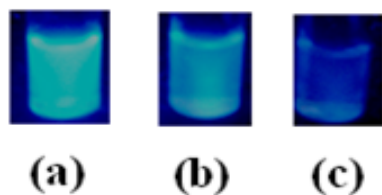


Figure 9S. Photographs of color change of (a) **1** ($c = 2.5 \times 10^{-5}$ M) and with 15 equiv. amounts of (b) $\text{HP}_2\text{O}_7^{3-}$ ($c = 1 \times 10^{-3}$ M) and (c) H_2PO_4^- ($c = 1 \times 10^{-3}$ M) under UV illumination.

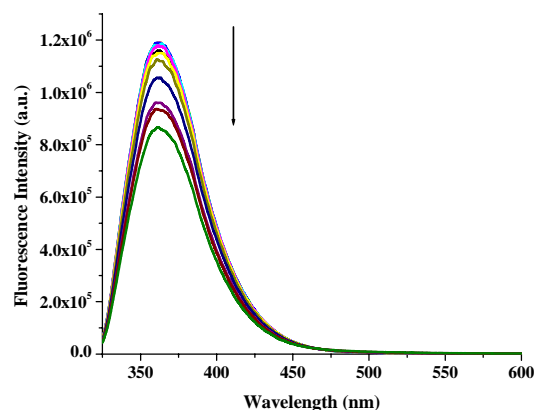


Figure 10S. Change in emission of receptor **2** ($c = 2.21 \times 10^{-5}$ M) upon addition of 15 equiv. amounts of H_2PO_4^- ($c = 1 \times 10^{-3}$ M) in CH_3CN containing 0.01% DMSO.

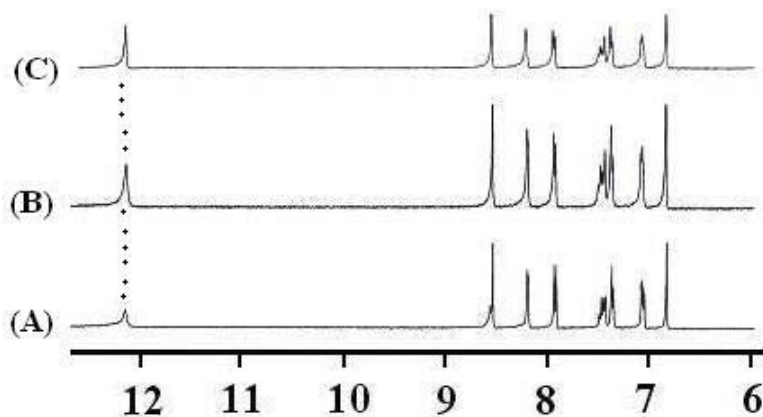


Figure 11S. Partial ^1H NMR (400 MHz) of **1** ($c = 5.01 \times 10^{-3}$ M) in the absence (A) and presence of 1 equiv (B) and 2 equiv (C) amounts of tetrabutylammonium dihydrogenphosphate in d_6 -DMSO.

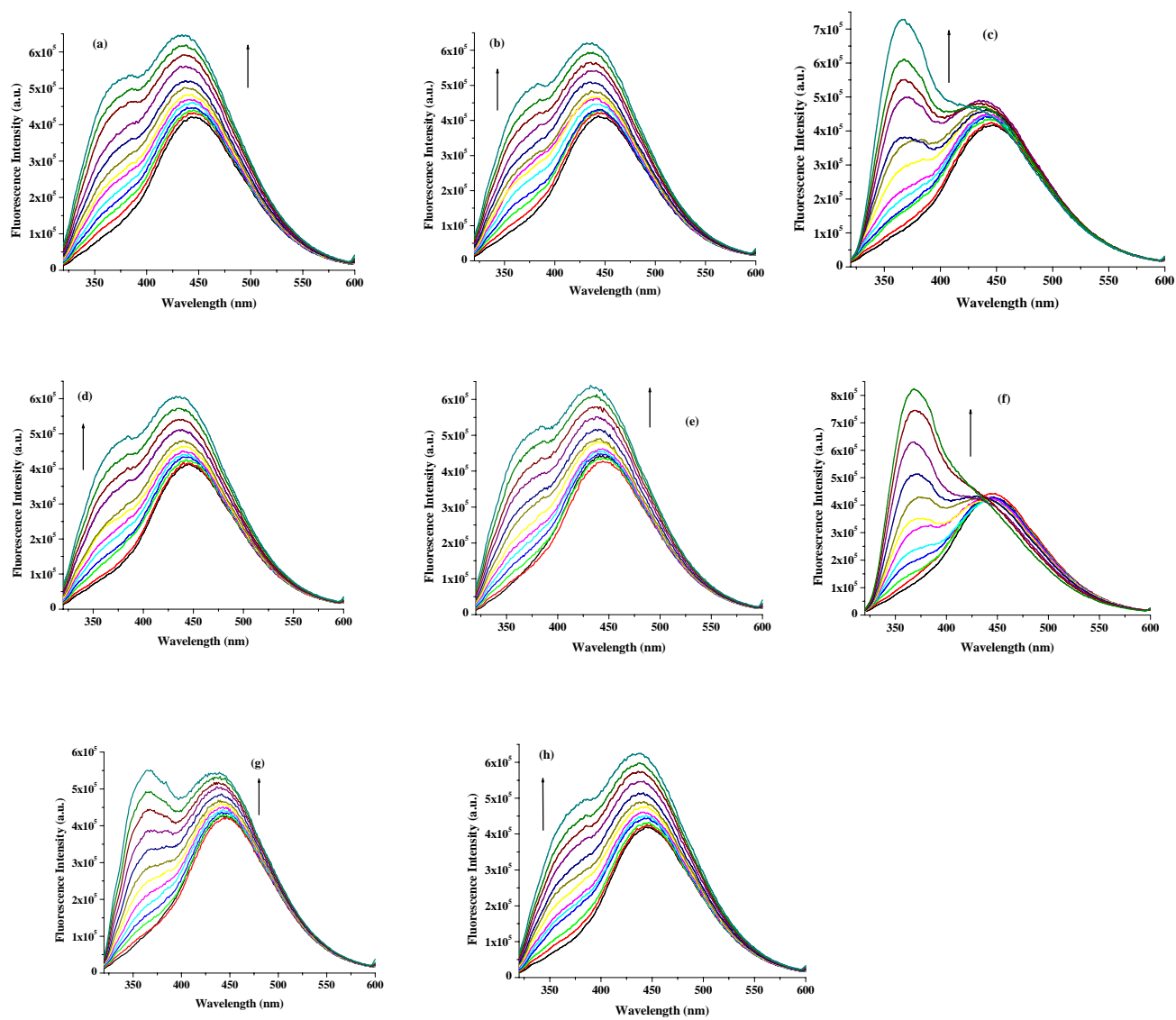


Figure 12S. Change in emission of **3** ($c = 5.01 \times 10^{-5}$ M) upon addition of (a) Cl⁻, (b) Br⁻, (c) F⁻, (d) I⁻, (e) HSO₄⁻, (f) HP₂O₇³⁻, (g) AcO⁻, (h) NO₃⁻ in CH₃CN containing 0.01% DMSO.

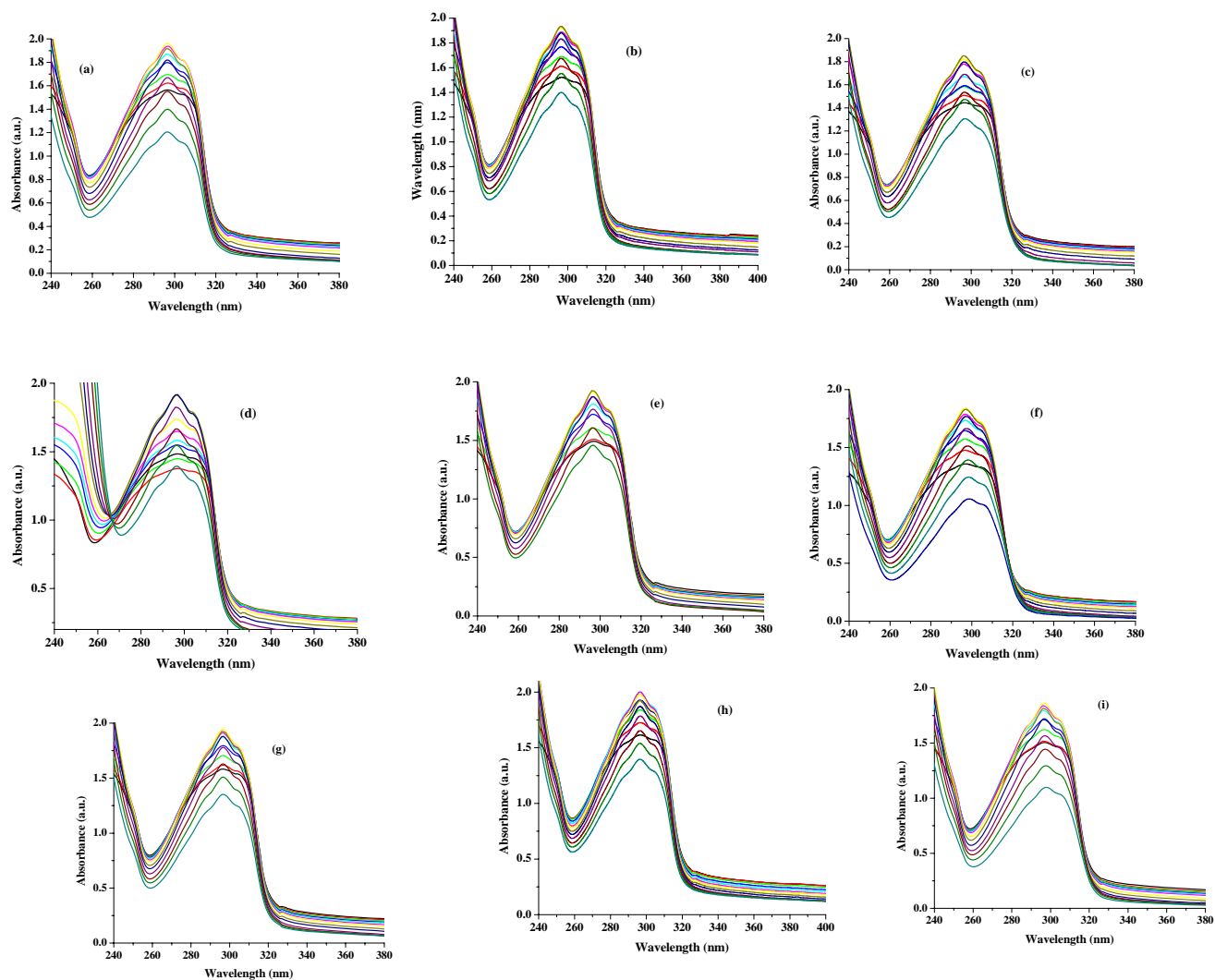


Figure 13S. Change in absorbance of **3** ($c = 5.01 \times 10^{-5}$ M) upon addition of (a) Cl^- , (b) Br^- , (c) F^- , (d) I^- , (e) HSO_4^- , (f) $\text{HP}_2\text{O}_7^{3-}$, (g) AcO^- , (h) NO_3^- , (i) H_2PO_4^- in CH_3CN containing 0.01% DMSO.

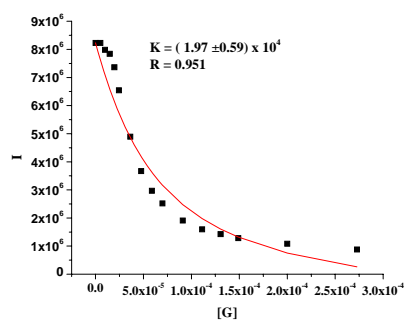


Figure 14S. Nonlinear binding constant curve for tetrabutylammonium dihydrogenphosphate ($c=1 \times 10^{-3} \text{ M}$) with receptor 1 ($c=2.25 \times 10^{-5} \text{ M}$) at 363 nm in CH_3CN containing 0.01% DMSO.

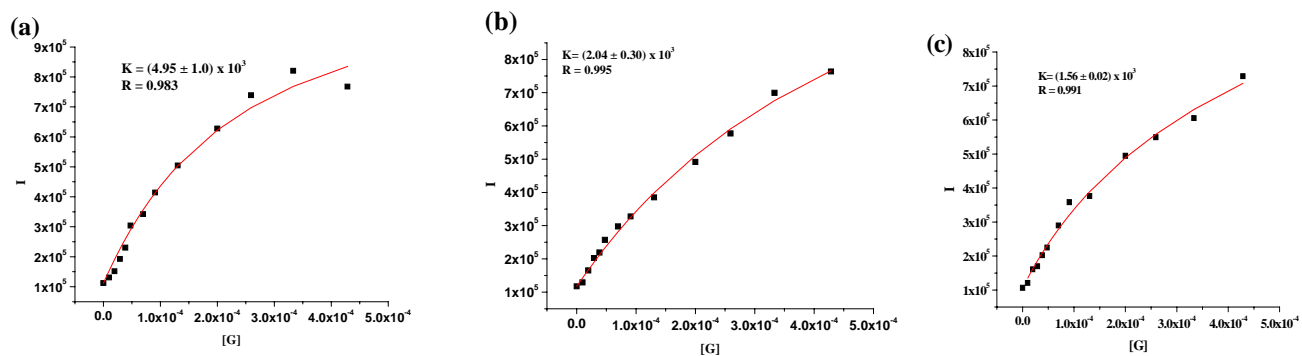


Figure 15S. Nonlinear binding constant curves for (a) tetrabutylammonium hydrogenpyrophosphate (b) tetrabutyl ammonium dihydrogenphosphate, (c) tetrabutylammonium fluoride ($c = 1 \times 10^{-3} \text{ M}$) with receptor 3 ($c = 5.01 \times 10^{-5} \text{ M}$) at 366 nm in CH_3CN containing 0.01% DMSO.

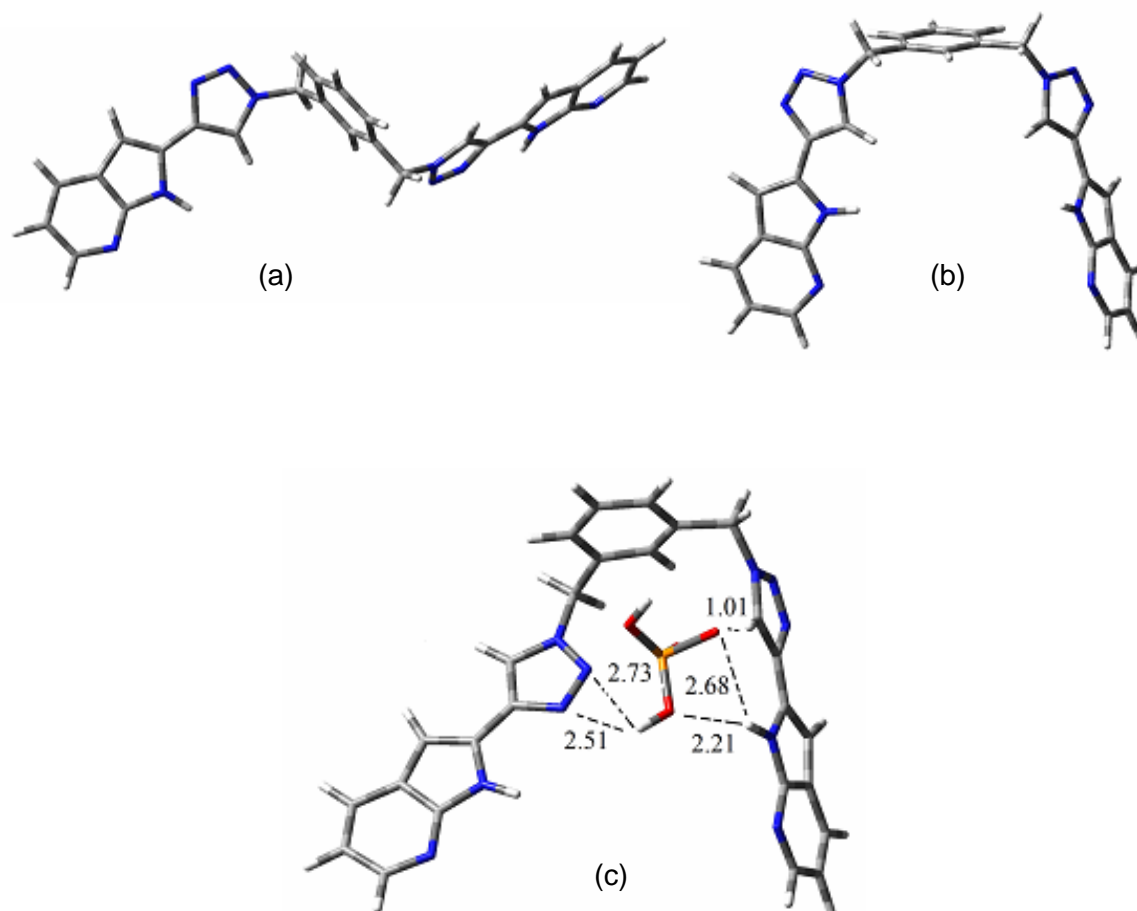
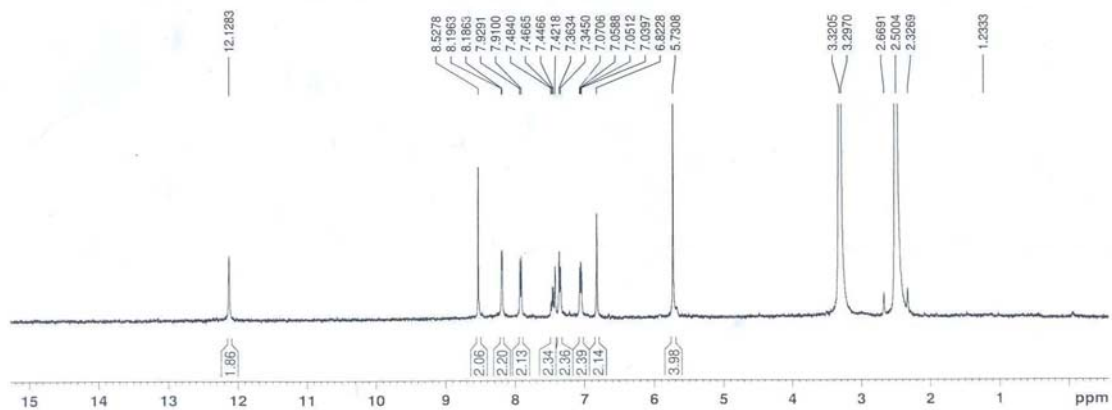
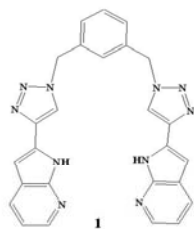
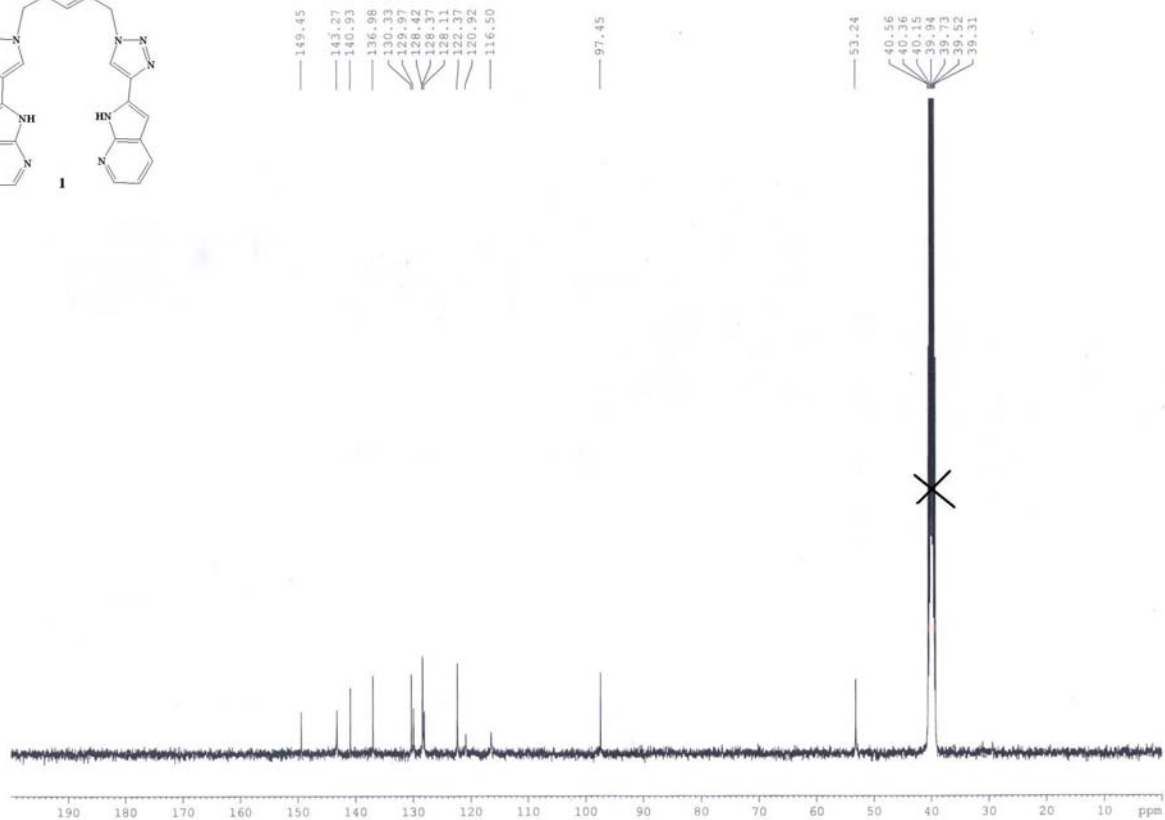
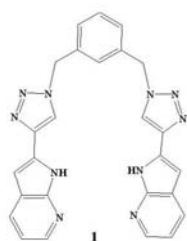


Figure 16S. PM6 optimized geometries of the (a) *anti*, (b) *syn* and (c) H_2PO_4^- complexed forms of **1**. Numerical values in the complex (c) indicate the hydrogen bond distances in Å and the *anti* form is stable by 3.01 kcal/mol over the *syn* form.

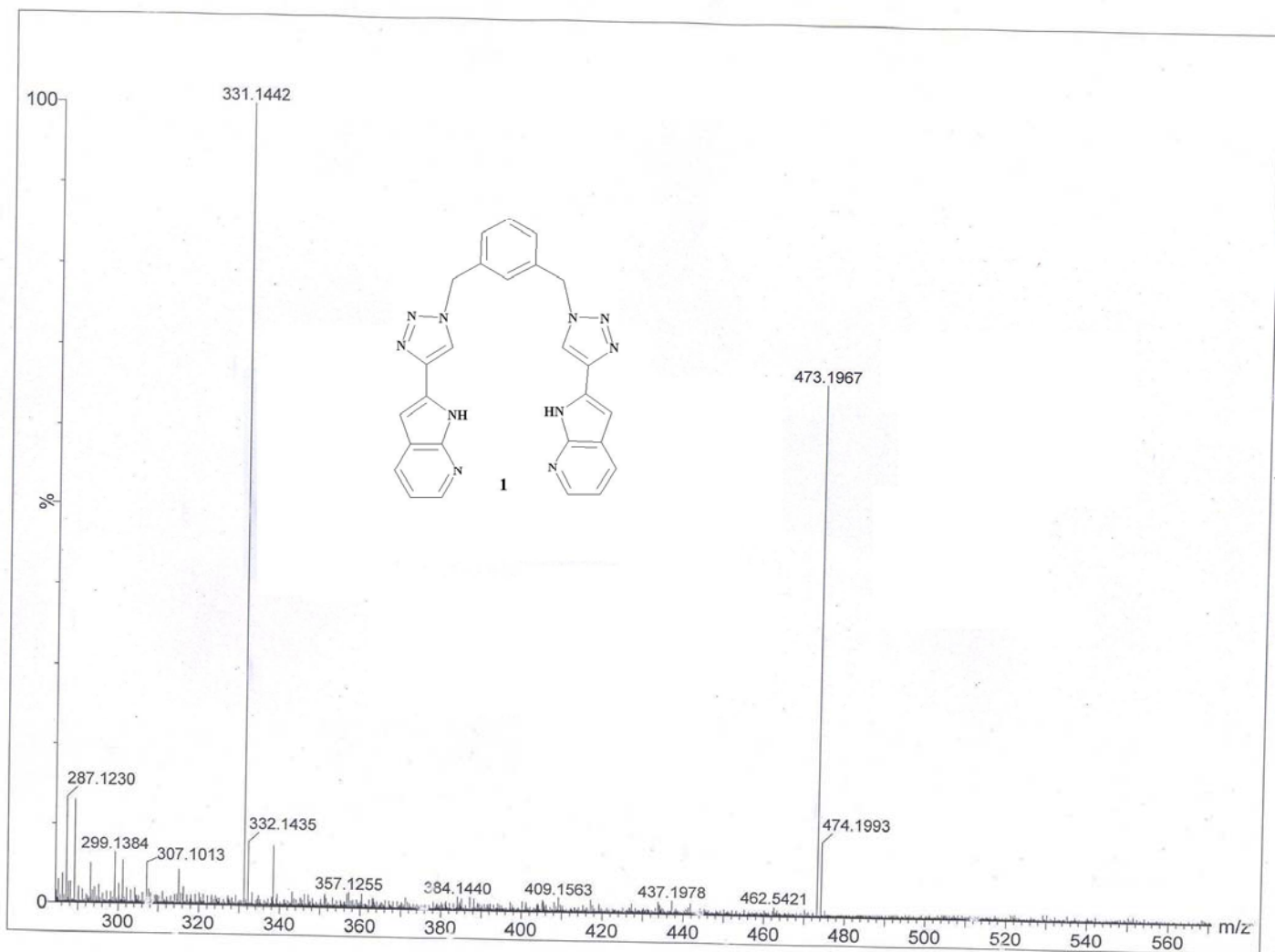
¹H NMR (400 MHz, d₆-DMSO)



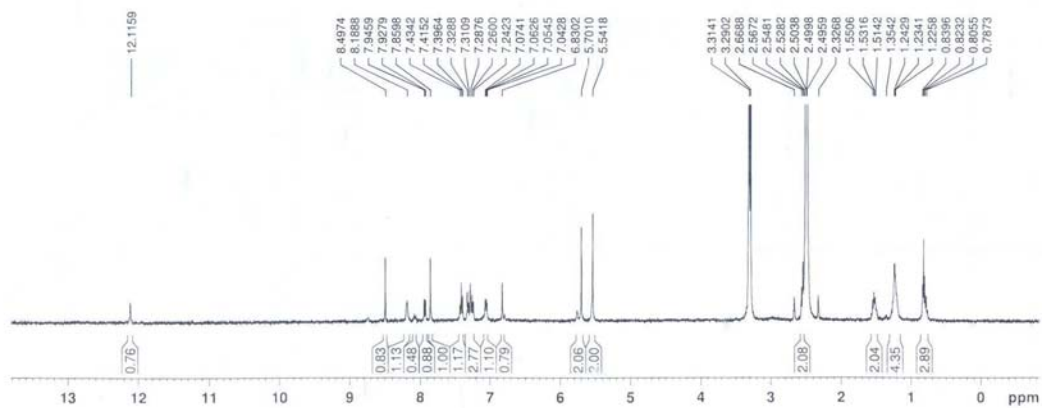
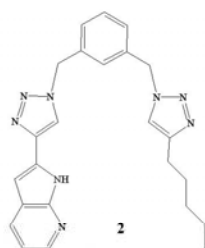
^{13}C NMR (100 MHz, $\text{d}_6\text{-DMSO}$)



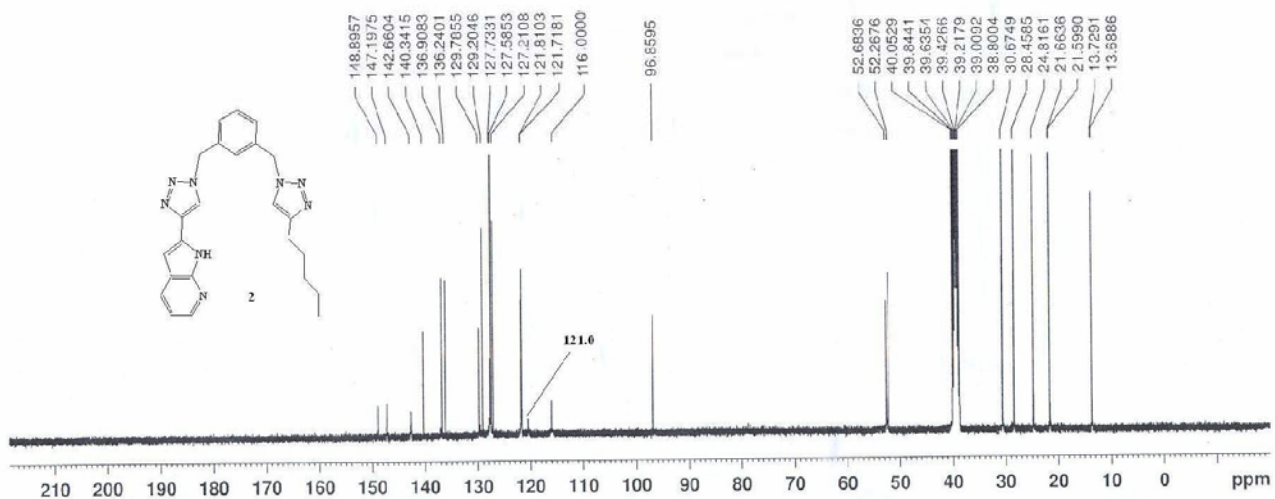
HRMS



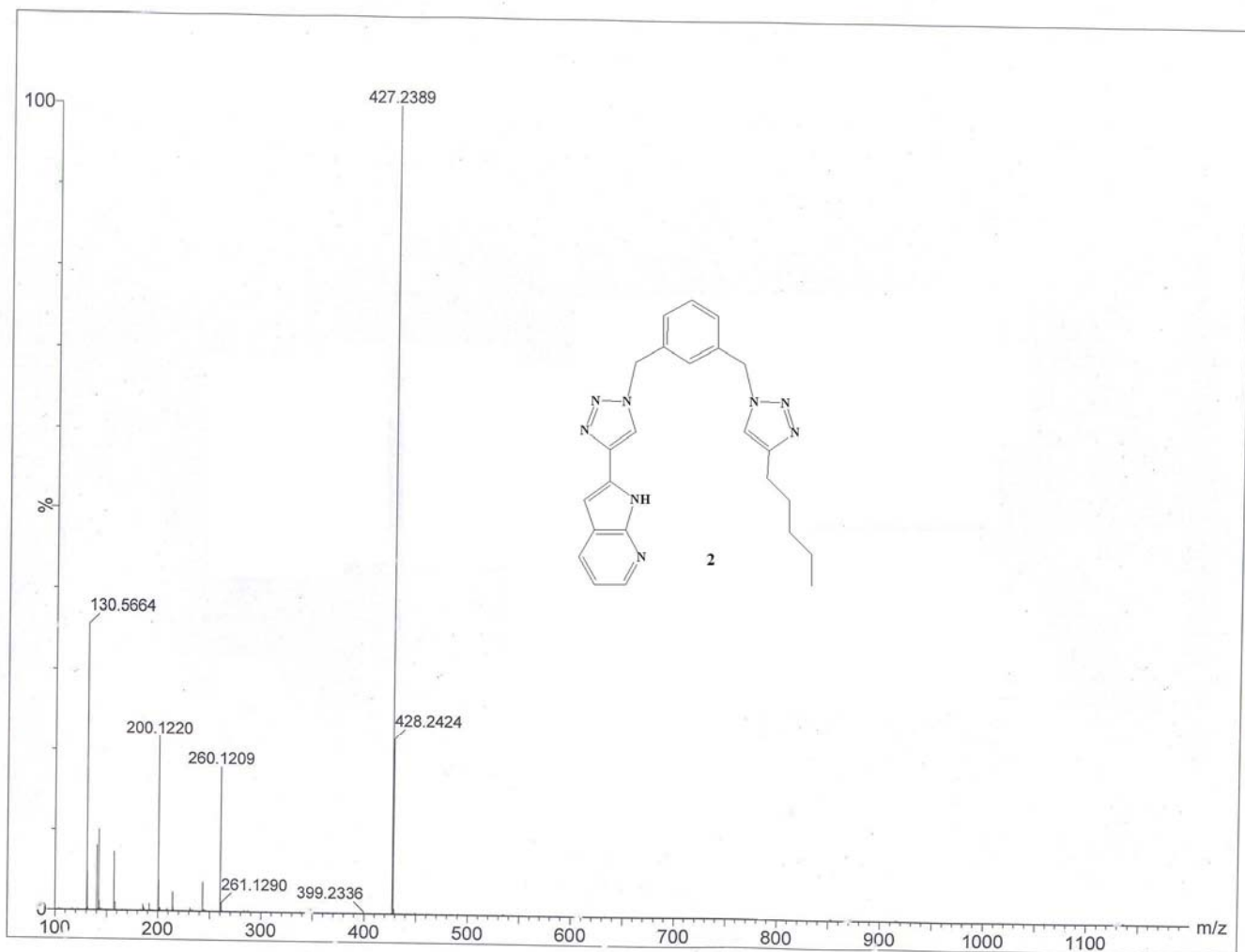
¹H NMR (400 MHz, d₆-DMSO)



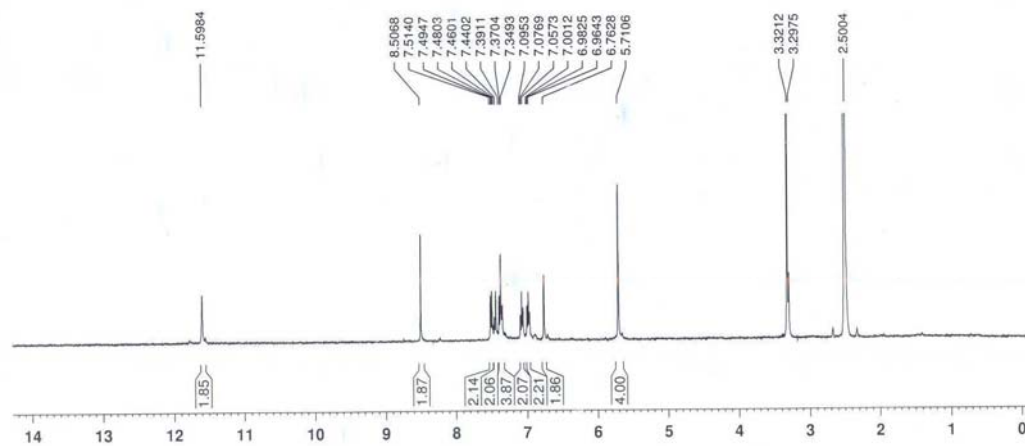
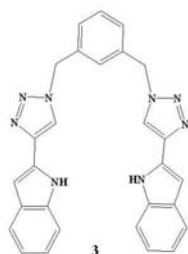
^{13}C NMR (100 MHz, $\text{d}_6\text{-DMSO}$)



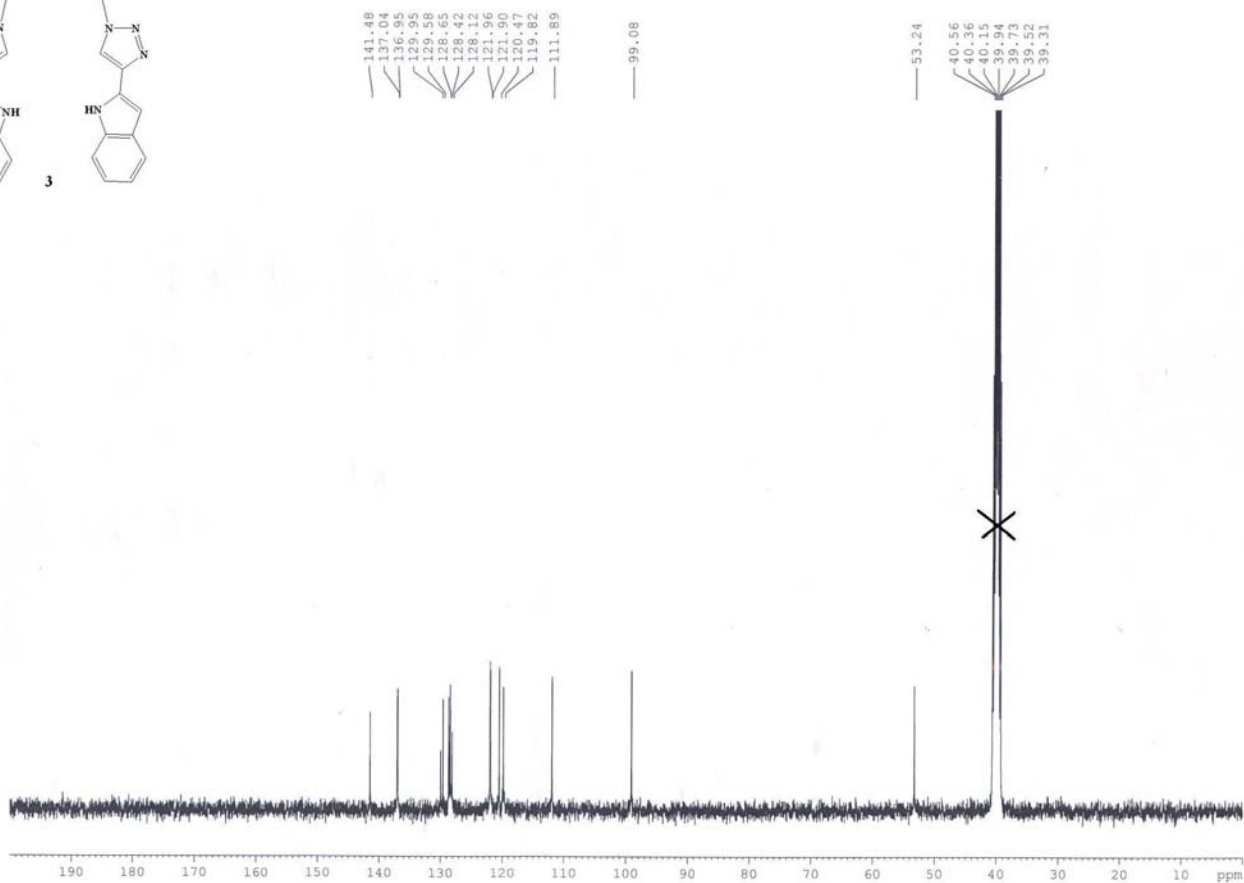
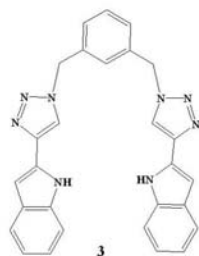
HRMS



^1H NMR (400 MHz, d_6 -DMSO)



^{13}C NMR (100 MHz, d_6 -DMSO)



HRMS

